

A study of charged κ in $J/\psi \rightarrow K^\pm K_S \pi^\mp \pi^0$

BES Collaboration

M. Ablikim¹, J. Z. Bai¹, Y. Bai¹, Y. Ban¹¹, X. Cai¹, H. F. Chen¹⁶, H. S. Chen¹,
 H. X. Chen¹, J. C. Chen¹, Jin Chen¹, X. D. Chen⁵, Y. B. Chen¹, Y. P. Chu¹,
 Y. S. Dai¹⁸, Z. Y. Deng¹, S. X. Du^{1a}, J. Fang¹, C. D. Fu¹, C. S. Gao¹,
 Y. N. Gao¹⁴, S. D. Gu¹, Y. T. Gu⁴, Y. N. Guo¹, Z. J. Guo^{15b}, F. A. Harris¹⁵,
 K. L. He¹, M. He¹², Y. K. Heng¹, H. M. Hu¹, T. Hu¹, G. S. Huang^{1c},
 X. T. Huang¹², Y. P. Huang¹, X. B. Ji¹, X. S. Jiang¹, J. B. Jiao¹², D. P. Jin¹,
 S. Jin¹, G. Li¹, H. B. Li¹, J. Li¹, L. Li¹, R. Y. Li¹, W. D. Li¹, W. G. Li¹,
 X. L. Li¹, X. N. Li¹, X. Q. Li¹⁰, Y. F. Liang¹³, B. J. Liu^{1d}, C. X. Liu¹, Fang Liu¹,
 Feng Liu⁶, H. M. Liu¹, J. P. Liu¹⁷, H. B. Liu^{4e}, J. Liu¹, Q. Liu¹⁵, R. G. Liu¹,
 S. Liu⁸, Z. A. Liu¹, F. Lu¹, G. R. Lu⁵, J. G. Lu¹, C. L. Luo⁹, F. C. Ma⁸,
 H. L. Ma², Q. M. Ma¹, M. Q. A. Malik¹, Z. P. Mao¹, X. H. Mo¹, J. Nie¹,
 S. L. Olsen¹⁵, R. G. Ping¹, N. D. Qi¹, J. F. Qiu¹, G. Rong¹, X. D. Ruan⁴,
 L. Y. Shan¹, L. Shang¹, C. P. Shen¹⁵, X. Y. Shen¹, H. Y. Sheng¹, H. S. Sun¹,
 S. S. Sun¹, Y. Z. Sun¹, Z. J. Sun¹, X. Tang¹, J. P. Tian¹⁴, G. L. Tong¹,
 G. S. Varner¹⁵, X. Wan¹, L. Wang¹, L. L. Wang¹, L. S. Wang¹, P. Wang¹,
 P. L. Wang¹, Y. F. Wang¹, Z. Wang¹, Z. Y. Wang¹, C. L. Wei¹, D. H. Wei³,
 N. Wu¹, X. M. Xia¹, G. F. Xu¹, X. P. Xu⁶, Y. Xu¹⁰, M. L. Yan¹⁶, H. X. Yang¹,
 M. Yang¹, Y. X. Yang³, M. H. Ye², Y. X. Ye¹⁶, C. X. Yu¹⁰, C. Z. Yuan¹,
 Y. Yuan¹, Y. Zeng⁷, B. X. Zhang¹, B. Y. Zhang¹, C. C. Zhang¹, D. H. Zhang¹,
 F. Zhang^{14f}, H. Q. Zhang¹, H. Y. Zhang¹, J. W. Zhang¹, J. Y. Zhang¹,
 X. Y. Zhang¹², Y. Y. Zhang¹³, Z. X. Zhang¹¹, Z. P. Zhang¹⁶, D. X. Zhao¹,
 J. W. Zhao¹, M. G. Zhao¹, P. P. Zhao¹, Z. G. Zhao¹⁶, B. Zheng¹, H. Q. Zheng¹¹,
 J. P. Zheng¹, Z. P. Zheng¹, B. Zhong⁹, L. Zhou¹, K. J. Zhu¹, Q. M. Zhu¹,
 X. W. Zhu¹, Y. S. Zhu¹, Z. A. Zhu¹, Z. L. Zhu³, B. A. Zhuang¹, B. S. Zou¹

¹ *Institute of High Energy Physics, Beijing 100049, People's Republic of China*

² *China Center for Advanced Science and Technology (CCAST), Beijing 100080, People's Republic of China*

³ *Guangxi Normal University, Guilin 541004, People's Republic of China*

⁴ *Guangxi University, Nanning 530004, People's Republic of China*

⁵ *Henan Normal University, Xinxiang 453002, People's Republic of China*

⁶ *Huazhong Normal University, Wuhan 430079, People's Republic of China*

⁷ *Hunan University, Changsha 410082, People's Republic of China*

⁸ *Liaoning University, Shenyang 110036, People's Republic of China*

⁹ *Nanjing Normal University, Nanjing 210097, People's Republic of China*

¹⁰ *Nankai University, Tianjin 300071, People's Republic of China*

¹¹ *Peking University, Beijing 100871, People's Republic of China*

¹² *Shandong University, Jinan 250100, People's Republic of China*

¹³ *Sichuan University, Chengdu 610064, People's Republic of China*

¹⁴ *Tsinghua University, Beijing 100084, People's Republic of China*

¹⁵ *University of Hawaii, Honolulu, HI 96822, USA*

¹⁶ *University of Science and Technology of China, Hefei 230026, People's Republic*

of China

¹⁷ Wuhan University, Wuhan 430072, People's Republic of China

¹⁸ Zhejiang University, Hangzhou 310028, People's Republic of China

^a Currently at: Zhengzhou University, Zhengzhou 450001, People's Republic of China

^b Currently at: Johns Hopkins University, Baltimore, MD 21218, USA

^c Currently at: University of Oklahoma, Norman, OK 73019, USA

^d Currently at: University of Hong Kong, Pok Fu Lam Road, Hong Kong

^e Currently at: Graduate University of Chinese Academy of Sciences, Beijing 100049, People's Republic of China

^f Currently at: Harbin Institute of Technology, Harbin 150001, People's Republic of China

Keywords: Charged κ , Low mass scalar, SU(3) symmetry breaking, J/ψ decays

Abstract

Based on 58×10^6 J/ψ events collected by BESII, the decay $J/\psi \rightarrow K^\pm K_S \pi^\mp \pi^0$ is studied. In the invariant mass spectrum recoiling against the charged $K^*(892)^\pm$, the charged κ particle is found as a low mass enhancement. If a Breit-Wigner function of constant width is used to parameterize the κ , its pole locates at $(849 \pm 77^{+18}_{-14}) - i(256 \pm 40^{+46}_{-22})$ MeV/ c^2 . Also in this channel, the decay $J/\psi \rightarrow K^*(892)^+ K^*(892)^-$ is observed for the first time. Its branching ratio is $(1.00 \pm 0.19^{+0.11}_{-0.32}) \times 10^{-3}$.

1 Introduction

The σ and κ are controversial particles in hadron spectroscopy. They were first found in the analysis of $\pi\pi$ and πK scattering data. Because the total phase shifts in the lower mass region are much less than 180° and they do not fit into ordinary $q\bar{q}$ meson nonets, they have been the subject of violent debates. Refs. ([1] - [12]) are some recent analyses that support their existence.

Evidence for κ particles comes from the study of production processes and the re-analysis of $K\pi$ scattering data. Evidence for the κ has been found in $D^+ \rightarrow K^- \pi^+ \pi^-$ [8], $J/\psi \rightarrow \bar{K}^*(892)^0 K^+ \pi^-$ [2,6], and $D^+ \rightarrow K^- \pi^+ \mu^+ \nu$ [13]. A $K\pi$ s-wave component is found in $D^0 \rightarrow K^- K^+ \pi^0$ [14], $D^+ \rightarrow K^- \pi^+ e^+ \nu_e$ [15], and $\tau \rightarrow K_S \pi^- \nu_\tau$ [16]. But no evidence for the κ in $D^0 \rightarrow K^- \pi^+ \pi^0$ [17] or for the charged κ in $D^0 \rightarrow K^- K^+ \pi^0$ [18] is seen. The κ is found in the phenomenological analysis of $K\pi$ scattering phase shift data ([12], [19] - [26]). However, some theorists are not convinced by the evidence ([27] - [30]). The

present status of the κ is summarized by the Particle Data Group PDG [31].

The σ and κ particles have been studied with BES data, where evidence for σ and κ particles is quite clear ([1] - [6]). A neutral κ was found in the decay $J/\psi \rightarrow \bar{K}^*(892)^0 \kappa^0 \rightarrow \bar{K}^*(892)^0 K^+ \pi^-$ [2,6]. Because of isospin symmetry, if a neutral κ exists, a charged κ should exist and could be produced in $J/\psi \rightarrow \bar{K}^*(892)^\pm \kappa^\mp$.

In this study, we search for and study the charged κ in $J/\psi \rightarrow K^\pm K_S \pi^\mp \pi^0$. Our analysis is based on 58 million J/ψ decays collected by BESII at the BEPC (Beijing Electron Positron Collider). BESII is a large solid-angle magnetic spectrometer which is described in detail in Ref. [32]. The momentum of charged particles is determined by a 40-layer cylindrical main drift chamber (MDC). Particle identification is accomplished using specific ionization (dE/dx) measurements in the MDC and time-of-flight (TOF) information in a barrel-like array of 48 scintillation counters. Outside of the TOF is a barrel shower counter (BSC) which measures the energy and direction of photons.

2 Event selection

In the event selection, candidate tracks are required to have a good track fit with the point of closest approach of the track to the beam axis being within the interaction region of 2 cm in r_{xy} and ± 20 cm in z (the beam direction), polar angles θ satisfying $|\cos \theta| < 0.80$, and transverse momenta $P_t > 50$ MeV/ c . Photons are required to be isolated from charged tracks, to come from the interaction region, and have deposited energy in the BSC greater than 40 MeV. Events are required to have four good charged tracks with total charge zero and at least two good photons.

For the K_S reconstruction, we loop over all oppositely charged pairs of tracks, assuming them to be pions, and fit them to $K_S \rightarrow \pi^+ \pi^-$, which determines vertices and $\pi^+ \pi^-$ invariant masses, $M_{\pi\pi}$, for the four possible combinations. The combination with $M_{\pi\pi}$ closest to M_{K_S} is selected and is required to satisfy $|M_{\pi^+ \pi^-} - M_{K_S}| < 20$ MeV/ c^2 and have its decay vertex in the xy -plane satisfy $r_{xy} > 0.008$ m. After K_S selection, the particle type of the remaining two tracks, that is whether they are $K^+ \pi^-$ or $K^- \pi^+$, is decided by selecting the combination with smallest $\chi_{TOF}^2 + \chi_{DEDX}^2$.

A four constraint (4C) kinematic fit is applied under the $K^\pm \pi^\mp \pi^+ \pi^- \gamma \gamma$ hypothesis, and $\chi_{4C}^2 < 20$ is required. Events with a $\gamma \gamma$ invariant mass satisfying $|M_{\gamma\gamma} - M_{\pi^0}| < 40$ MeV/ c^2 are fitted with a 5C kinematic fit to $K^\pm \pi^\mp \pi^+ \pi^- \pi^0$ with the two photons constrained to the π^0 mass, and events with $\chi_{5C}^2 < 50$ are selected. The $\pi^\mp \pi^0$ mass distribution is shown in Fig. 1(a), where the

ρ is clearly seen. Decays with an intermediate ρ are background, and the requirement $|M_{\pi^+\pi^0} - M_\rho| > 100 \text{ MeV}/c^2$ is applied to remove them. The requirements $|M_{K_S\pi^0} - 0.897| > 40 \text{ MeV}/c^2$ and $|M_{K^\pm\pi^\mp} - 0.897| > 40 \text{ MeV}/c^2$ are used to remove backgrounds from $J/\psi \rightarrow K^*(892)^0 K^\pm\pi^\mp$ and $J/\psi \rightarrow K^*(892)^0 K_S\pi^0$. After these requirements, the combined $K^\pm\pi^0$ and $K_S\pi^\mp$ mass distribution is shown in Fig. 1(b); the highest narrow peak is charged $K^*(892)$. The $M_{K^\pm\pi^0}$ versus $M_{K_S\pi^\mp}$ scatter plot is shown in Fig. 1(c). There are two clear bands, a vertical and horizontal band, which correspond to $J/\psi \rightarrow K^*(892)^\pm K_S\pi^\mp$ and $J/\psi \rightarrow K^*(892)^\pm K^\mp\pi^0$, respectively. The requirements $|M_{K^\pm\pi^0} - 0.892| < 80 \text{ MeV}/c^2$ and $|M_{K_S\pi^\pm} - 0.892| < 80 \text{ MeV}/c^2$ are imposed to select $J/\psi \rightarrow K^*(892)^\pm K_S\pi^\mp$ and $J/\psi \rightarrow K^*(892)^\pm K^\mp\pi^0$ events, respectively.

After the above selection, the combined $K_S\pi^\mp$ and $K^\mp\pi^0$ invariant mass distribution recoiling against the $K^*(892)^\pm$ is shown in Fig. 1(d). It is the sum of the four decays listed in Table 1 with about 1000 events for each, as listed in the table, and a total of 4121 events. In Fig. 1(d), a clear narrow peak at 892 MeV/c^2 and a wider peak at about 1430 MeV/c^2 are seen. In addition, there is a broad low mass enhancement just above threshold. The spectrum is quite similar to the spectrum of $K^+\pi^-$ in the decay $J/\psi \rightarrow \bar{K}^*(892)^0 K^+\pi^-$ [6]. The biggest difference between them is that the charged $K^*(892)$ peak is much larger than the neutral $K^*(892)$ peak. The $K^*(892)\pi$ invariant mass distribution is shown in Fig. 1(e), where there are indications of peaks at 1270 MeV/c^2 and 1400 MeV/c^2 . The resulting Dalitz plot is shown in Fig. 1(f). The two diagonal bands correspond to the low mass enhancement combined with the 892 MeV/c^2 peak and the peak around 1430 MeV/c^2 in the $K\pi$ spectrum.

Channel	Events
$J/\psi \rightarrow K^*(892)^+ K_S\pi^- \rightarrow K^+\pi^0 K_S\pi^-$	1023
$J/\psi \rightarrow K^*(892)^- K_S\pi^+ \rightarrow K^-\pi^0 K_S\pi^+$	946
$J/\psi \rightarrow K^*(892)^+ K^-\pi^0 \rightarrow K_S\pi^+ K^-\pi^0$	1055
$J/\psi \rightarrow K^*(892)^- K^+\pi^0 \rightarrow K_S\pi^- K^+\pi^0$	1097

Table 1
Four signal channels and number of events from each.

3 Background Studies

Possible sources of background are studied. First, sideband backgrounds are studied. The $\pi^+\pi^-$ mass distribution is shown in Fig. 2(a), where a clear K_S signal can be seen and the background level is quite low. The $K\pi$ spectrum from K_S side-band events is shown in Fig. 2(b). (The K_S side-band is defined by $0.02 \text{ GeV}/c^2 < |M_{\pi\pi} - 0.497| < 0.04 \text{ GeV}/c^2$.) There are no clear structures. The $\gamma\gamma$ spectrum is shown in Fig. 2(c), and the $K\pi$ spectrum of the 284 π^0 side-

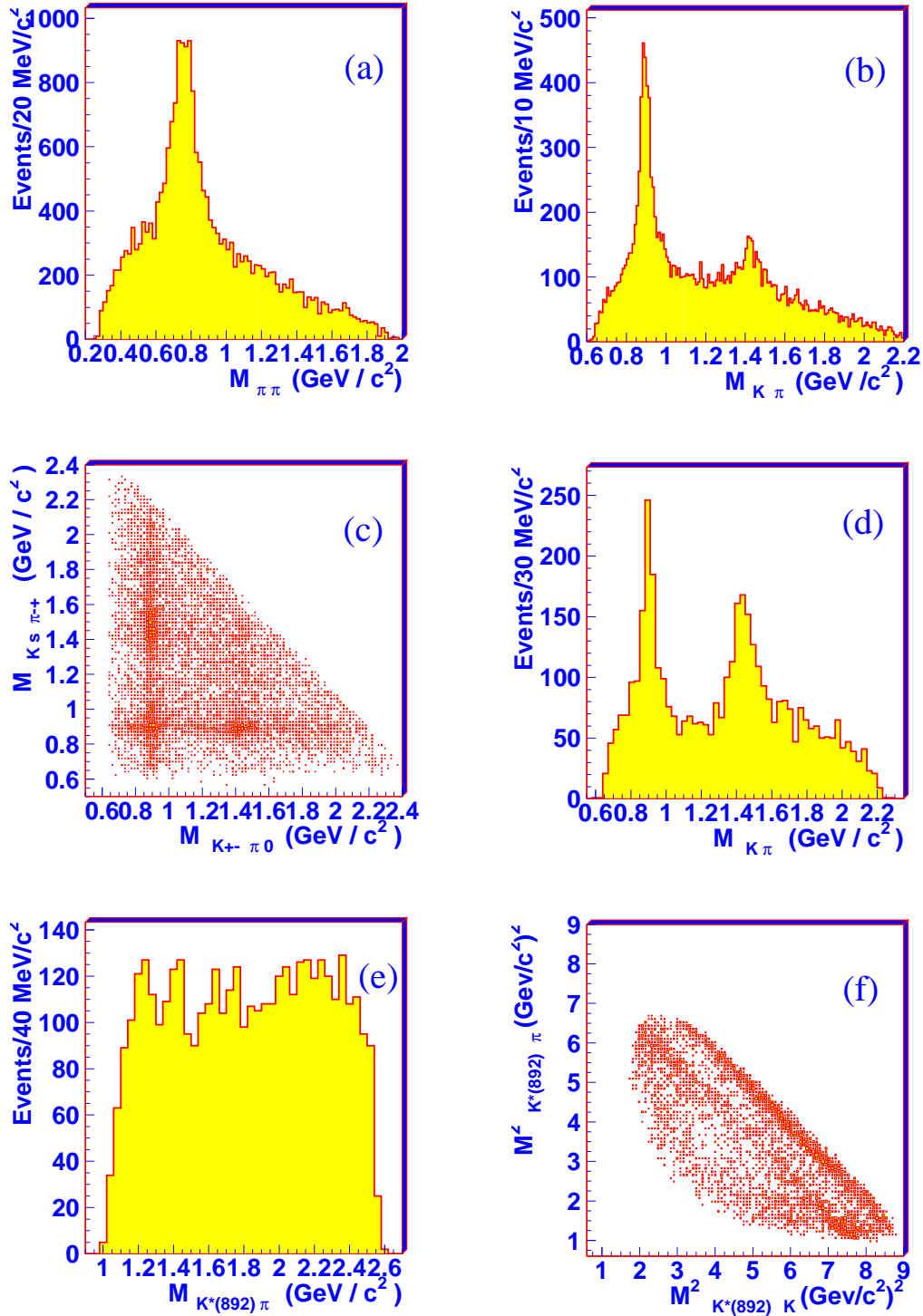


Fig. 1. (a) $\pi^{\mp}\pi^0$ mass distribution. (b) Combined $K^{\pm}\pi^0$ and $K_S\pi^{\mp}$ mass distribution after final cuts except the $K^*(892)$ cuts. (c) Scatter plot of $M_{K^{\pm}\pi^0}$ versus $M_{K_S\pi^{\mp}}$. (d) Invariant mass distribution of $K^{\pm}\pi^0$ and $K_S\pi^{\pm}$ recoiling against $K^*(892)^{\mp}$. (e) Invariant mass distribution of $K^*(892)\pi$. (f) Dalitz plot.

band events is shown in Fig. 2(d). (The π^0 sideband is defined by $0.04 \text{ GeV}/c^2 < |m_{\gamma\gamma} - 0.135| < 0.08 \text{ GeV}/c^2$.) The structures in Fig. 2(d) are similar to those in the signal region and come from signal events in the π^0 tails. The $K^*(892)$ side-band background is shown by the dark shaded histogram in Fig. 2(e). (The $K^*(892)$ side-band is defined by $0.08 \text{ GeV}/c^2 < |M_{K\pi} - 0.892| < 0.16 \text{ GeV}/c^2$.) The clear $K^*(892)$ in the $K\pi$ mass distribution of $K^*(892)$ side-band events mainly comes from the cross channel. (There are two bands in the scatter plot in Fig. 1(c). When we select one band, we will also select some events from the other band where it crosses the first band. These events correspond to cross channel background.) Fig. 2(f) shows the $K\pi$ spectrum after side-band subtraction. The low mass enhancement and $K^*(892)$ peak survive after side-band subtraction.

Next, we perform Monte Carlo simulation to study the main physics background processes, including $J/\psi \rightarrow \gamma\eta_c \rightarrow \gamma K^* \bar{K}^* \rightarrow \gamma K^\pm K_S \pi^\mp \pi^0$, $J/\psi \rightarrow \gamma\eta_c \rightarrow \gamma K^*(892)^\pm K^\mp \pi^0 \rightarrow \gamma K^\pm K_S \pi^\mp \pi^0$, $J/\psi \rightarrow \gamma\eta_c \rightarrow \gamma K^*(892)^\pm K_S \pi^\mp \rightarrow \gamma K^\pm K_S \pi^\mp \pi^0$, $J/\psi \rightarrow \pi^0 \pi^+ \pi^- \pi^+ \pi^-$, and $J/\psi \rightarrow \pi^0 K^+ K^- \pi^+ \pi^-$. The selection efficiencies are much lower than 1%, and the largest number of background events contributed is about 6. Therefore, the physics background is quite low.

4 Partial wave analysis

A partial wave analysis (PWA), which is based on the covariant helicity amplitude analysis ([33] - [37]), is performed for the charged κ . We add the likelihoods of all four channels together, and find the minimum of the sum. This is the same method as used to fit $J/\psi \rightarrow K^*(892)^0 K^+ \pi^-$ [6]. The main difference here is that the decay $J/\psi \rightarrow K^*(892)^\pm K^*(892)^\mp$ is included in the fit.

In the PWA analysis, ten resonances, κ , $K_0^*(1430)$, IPS , $K_2^*(1430)$, $K_2^*(1920)$, $K^*(1410)$ and $K^*(892)$ in the $K\pi$ spectrum, $K_1(1270)$ and $K_1(1400)$ in the $K^*(892)\pi$ spectrum, and $b_1(1235)$ in the $K^*(892)K$ spectrum, and two backgrounds, listed as the last items in Table 2, are considered in the fit. In Table 2, IPS (Interference Phase Space) refers to a broad 0^+ structure with a $K\pi$ invariant mass spectrum the same as phase space, that interferes with κ . K^* BG refers to the $K^*(892)$ background coming from the cross channel. PS (Phase Space) refers to the background with no interference with resonances and with a shape almost the same as that of phase space.

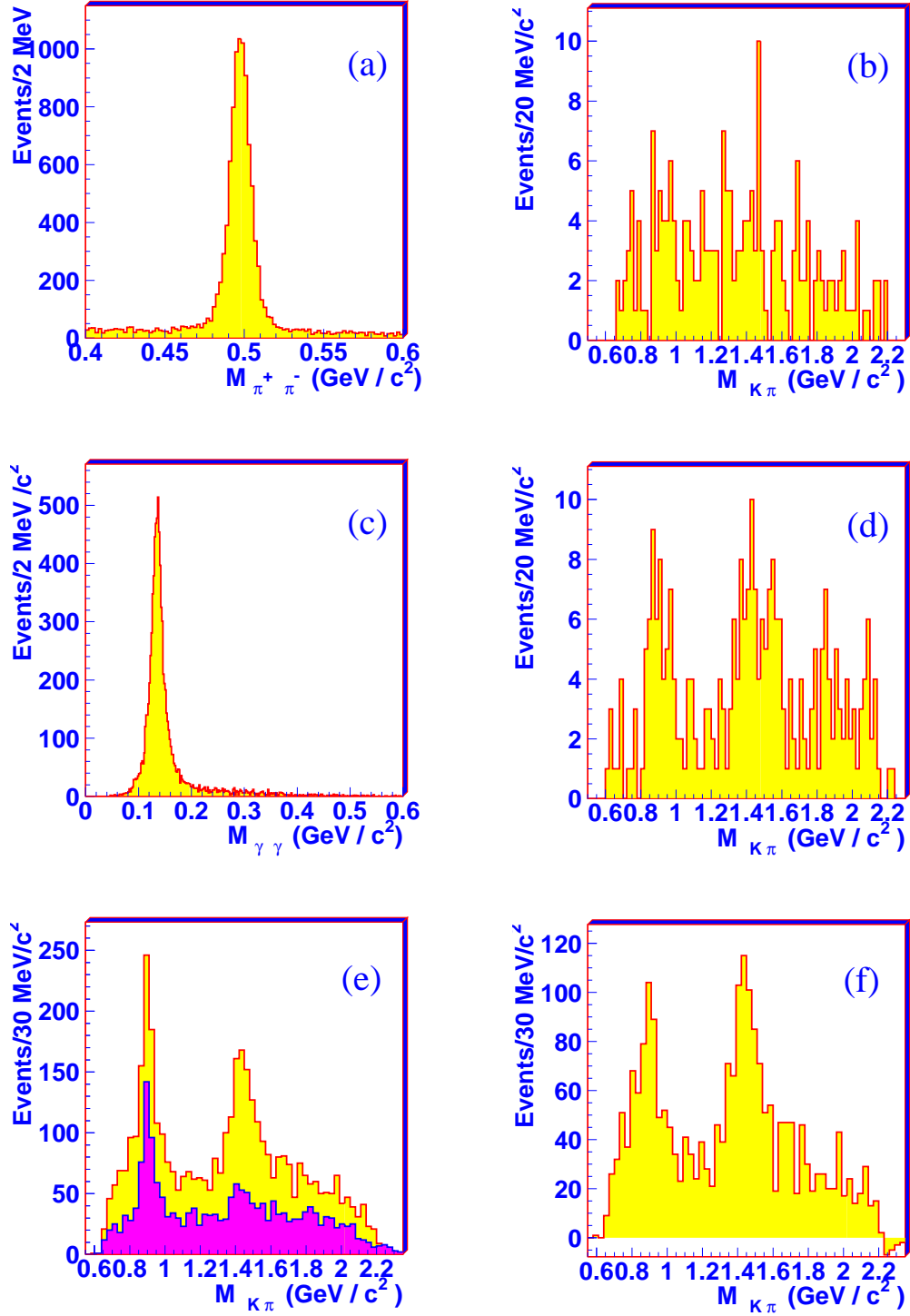


Fig. 2. (a) $m_{\pi^+\pi^-}$ mass distribution after final event selection except for the K_S requirement. (b) K_S side-band structure. (c) $m_{\gamma\gamma}$ mass distribution after final data selection except the π^0 requirement. (d) $M_{K\pi}$ distribution from π^0 side-band events. (e) $K\pi$ spectrum recoiling against $K^*(892)$. The dark shaded histogram is from K^* side-band events. (f) The $K\pi$ spectrum after side-band subtraction.

Resonance	Spin-Parity	Decay Mode	Mass (MeV// c^2)	Width (MeV/ c^2)	Sig.
κ (1)	0^+	$K\pi$	$810 \pm 68_{-24}^{+15}$	$536 \pm 87_{-47}^{+106}$	$> 6\sigma$
κ (2)	0^+	$K\pi$	$884 \pm 40_{-22}^{+11}$	$478 \pm 77_{-41}^{+71}$	$> 6\sigma$
κ (3)	0^+	$K\pi$	$1165 \pm 58_{-41}^{+120}$	$1349 \pm 500_{-176}^{+472}$	$> 6\sigma$
$K_0^*(1430)$	0^+	$K\pi$	1400 ± 86	325 ± 200	0.6σ
IPS	0^+	$K\pi$	—	—	$> 6\sigma$
$K_2^*(1430)$	2^+	$K\pi$	1411 ± 30	111 ± 46	$> 6\sigma$
$K_2^*(1920)$	2^+	$K\pi$	2020 ± 140	705 ± 160	$> 6\sigma$
$K^*(1410)$	1^-	$K\pi$	1420 ± 14	130 ± 28	$> 6\sigma$
$K^*(892)$	1^-	$K\pi$	896 ± 8	57 ± 12	$> 6\sigma$
$K_1(1270)$	1^+	$K^*(892)\pi$	1254 ± 14	60 ± 28	$> 6\sigma$
$K_1(1400)$	1^+	$K^*(892)\pi$	1390 ± 30	146 ± 44	$> 6\sigma$
$b_1(1235)$	1^+	$K^*(892)K$	1230 ± 52	142 ± 38	4.5σ
$K^*(892)$ BG	1^-	$K\pi$	—	—	$> 6\sigma$
PS BG	—	—	—	—	—

Table 2

Resonances included in the fit of this channel. Masses and widths of various resonances are determined by mass and width scans. κ (1), (2) and (3) are results given by fits using Breit-Wigner functions (1), (2) and (3) to fit κ respectively. IPS refers to the broad 0^+ structure which interferes with κ . K^* BG refers to the $K^*(892)$ background coming from the cross channel. PS BG refers to the background with no interference with resonances.

Three different parameterizations are used to fit the κ . They are

$$BW_\kappa = \frac{1}{m_\kappa^2 - s - im_\kappa\Gamma_\kappa}, \quad \Gamma_\kappa = \text{constant}, \quad (1)$$

$$BW_\kappa = \frac{1}{m_\kappa^2 - s - i\sqrt{s}\Gamma_\kappa(s)}, \quad \Gamma_\kappa(s) = \frac{g_\kappa^2 \cdot k_\kappa}{8\pi s}, \quad (2)$$

$$BW_\kappa = \frac{1}{m_\kappa^2 - s - i\sqrt{s}\Gamma_\kappa(s)}, \quad \Gamma_\kappa(s) = \alpha \cdot k_\kappa, \quad (3)$$

where k_κ is the magnitude of the K momentum in the $K\pi$, or the κ , center of mass system [38], and α is a constant which will be determined by the fit. Parameters in the Breit-Wigner function are determined by mass and width scans. The minima of the scan curves give the central values of mass and width parameters. From these, the corresponding Breit-Wigner pole positions can be directly calculated from equation (1), (2) and (3). Our final results are listed in Table 3, where the first errors are statistical, and the second are systematic. The mass and width parameters obtained by different parameterizations are quite different, but their poles are almost the same, which is quite similar to what was found in the study of the neutral κ . The results for the neutral κ [6]

are shown in Table 4 and are consistent with the charged κ .

	BW (1)	BW (2)	BW (3)
Mass (MeV/ c^2)	$810 \pm 68^{+15}_{-24}$	$884 \pm 40^{+11}_{-22}$	$1165 \pm 58^{+120}_{-41}$
Width (MeV/ c^2)	$536 \pm 87^{+106}_{-47}$	$478 \pm 77^{+71}_{-41}$	$1349 \pm 500^{+472}_{-176}$
pole (MeV/ c^2)	$(849 \pm 77^{+18}_{-14})$ $-i(256 \pm 40^{+46}_{-22})$	$(849 \pm 51^{+14}_{-28})$ $-i(288 \pm 101^{+64}_{-30})$	$(839 \pm 145^{+24}_{-7})$ $-i(297 \pm 51^{+50}_{-18})$

Table 3

Masses, widths and pole positions of the charged κ . In the table, the first errors are statistical, and the second are systematic. BW (1) means equation (1) is used to fit the κ . BW (2) and BW (3) have similar meanings.

	BW (1)	BW (2)	BW (3)
Mass (MeV/ c^2)	$745 \pm 26^{+14}_{-91}$	$874 \pm 25^{+12}_{-55}$	$1140 \pm 39^{+47}_{-80}$
Width (MeV/ c^2)	$622 \pm 77^{+61}_{-78}$	$518 \pm 65^{+27}_{-87}$	$1370 \pm 156^{+406}_{-148}$
pole (MeV/ c^2)	$(799 \pm 37^{+16}_{-90})$ $-i(290 \pm 33^{+25}_{-38})$	$(836 \pm 38^{+18}_{-87})$ $-i(329 \pm 66^{+28}_{-46})$	$(811 \pm 74^{+17}_{-83})$ $-i(285 \pm 20^{+18}_{-42})$

Table 4

Masses, widths and pole positions of the neutral κ [6]. BW (1) means equation (1) is used to fit the κ . BW (2) and BW (3) have similar meaning.

Our final results correspond to the solution with the minimum least likelihood. Differences among solutions with similar likelihood values are included as systematic uncertainties. Also included are the effect of removing $K_0(1430)$, IPS, $b_1(1235)$ and $K^*(892)\bar{K}^*(892)$, the result of a fit with the $K^*(892)$ background level floating, and the result from a fit using direct side-band subtraction.

The masses and widths of all resonances obtained by mass and width scans are shown in Table 2. In the fit, the contribution from $K_0^*(1430)$ is small; its statistical significance is only 0.6σ . Because it is expected in this channel, it is included in the final solution. The $K\pi$ mass distribution is shown in Fig. 3(a), where points with error bars are data, and the light shaded histogram is the final fit. In the figure, the dark shaded histogram shows the contribution of the charged κ . Fig. 3(b) shows the fit for the $K^*(892)\pi$ spectrum, and Fig. 4 shows the angular distributions.

5 Branching ratio measurements

The decay $J/\psi \rightarrow K^*(892)^\pm \kappa^\mp$ contributes 655 events. Monte Carlo simulation of $J/\psi \rightarrow K^*(892)^\pm \kappa^\mp \rightarrow K^\pm K_S \pi^\mp \pi^0$ determines an efficiency of 2.33%, and the branching ratio of $J/\psi \rightarrow K^*(892)^+ \kappa^-$ or $J/\psi \rightarrow K^*(892)^- \kappa^+$ is

$$BR = \frac{655/4}{2.33\% \times 5.8 \times 10^7 \times 1/9} = (1.09 \pm 0.18^{+0.94}_{-0.54}) \times 10^{-3}, \quad (4)$$

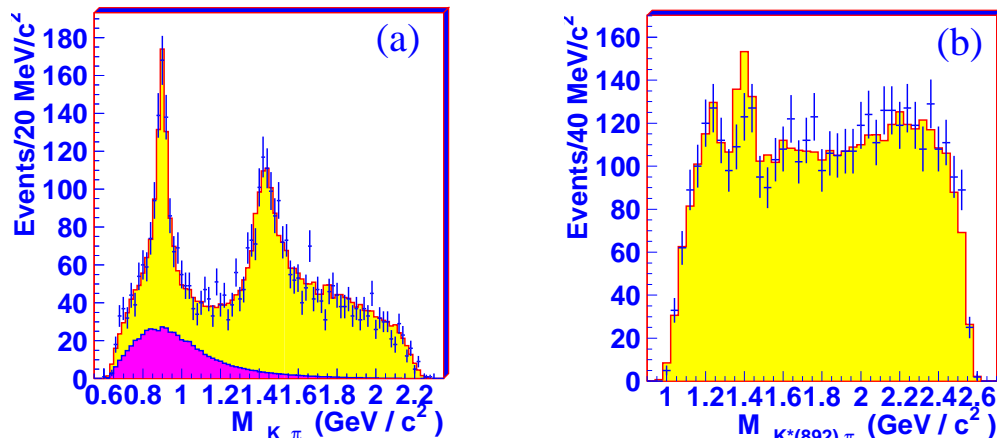


Fig. 3. (a) Final fit results for the $K\pi$ spectrum. Points with error bars are data, the light shaded histogram is the final global fit, and the dark shaded histogram is the contribution of the κ . (b) Final fit of $K^*(892)\pi$ spectrum. Dots with error bars are data, and the histogram is the final global fit. There are two peaks in the lower mass region. The lower one is fit by the $K_1(1270)$, and the higher one is by the $K_1(1400)$.

where, the first error is statistical, the second error is systematic, the factor $\frac{1}{4}$ is because the events are the sum of four channels, and $\frac{1}{9}$ is the isospin factor. In the previous study of the decay $J/\psi \rightarrow \bar{K}^*(892)^0 K^+ \pi^-$, the corresponding branching ratio for the neutral κ ¹ is $(0.52 - 0.97) \times 10^{-3}$. The two results are consistent with isospin symmetry. The systematic error includes uncertainties from multi-solutions, from different background fit methods, and from removing some components from the fit ($K_0^*(1430)$, IPS, $b_1(1235)$, and $K^*(892)^\pm K^*(892)^\mp$).

Also interesting is the existence of the J/ψ electromagnetic decay $J/\psi \rightarrow K^*(892)^\pm K^*(892)^\mp$. The peak at 892 MeV/ c^2 in the $K\pi$ invariant mass spectrum (see Fig. 1(d)) comes from both cross channel background and from $J/\psi \rightarrow K^*(892)^\pm K^*(892)^\mp$. The number of events from the cross channel can be calculated approximately from the $K^*(892)$ side-band structure, shown in Fig. 2(e), where the narrow peak at 892 MeV/ c^2 is clear. In the final fit, the decay $J/\psi \rightarrow K^*(892)^\pm K^*(892)^\mp$ contributes 323 events. The Monte Carlo simulation of the decay $J/\psi \rightarrow K^*(892)^\pm K^*(892)^\mp \rightarrow K^\pm K_S \pi^\mp \pi^0$ yields an efficiency of 1.25%, and the branching ratio of $J/\psi \rightarrow K^*(892)^+ K^*(892)^-$ is

$$BR = \frac{323/2}{1.25\% \times 5.8 \times 10^7 \times 1/9 \times 2} = (1.00 \pm 0.19_{-0.32}^{+0.11}) \times 10^{-3}, \quad (5)$$

¹ The branching ratio of the neutral κ was not reported in Ref. [6]. In the study of the neutral κ , the number of κ events was in the range 1891 - 3516, and the selection efficiency was 14.2%. Its branching ratio is $\frac{1891-3516}{14.2\% \times 5.8 \times 10^7 \times 4/9} = (0.52 - 0.97) \times 10^{-3}$

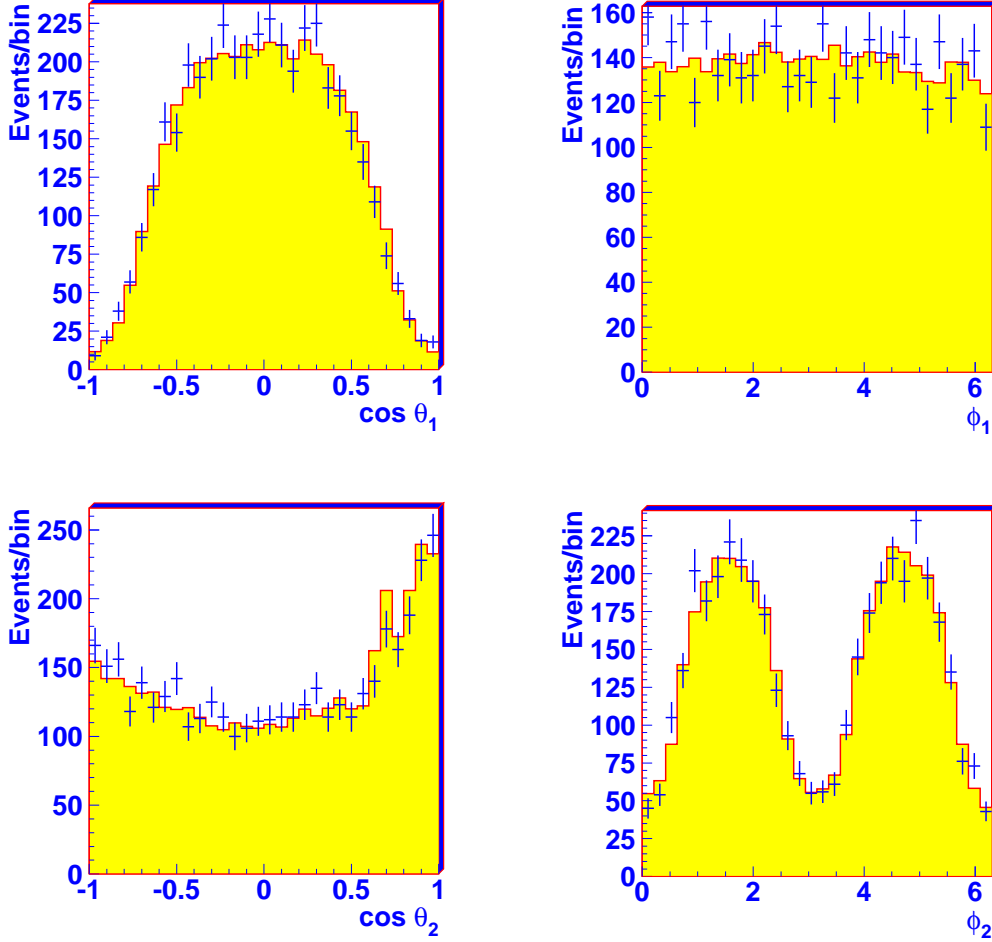


Fig. 4. Final fit result for the angular distributions. Dots with error bars are data, and the histogram is the final global fit. The upper left figure shows the final fit of the θ_1 distribution, the upper right shows the final fit of the ϕ_1 distribution, the lower left shows the final fit of the θ_2 distribution, the lower right shows the final fit of the ϕ_2 distribution. θ_1 and ϕ_1 are the polar angle and azimuthal angle of the $K\pi$ system in the J/ψ center of mass system. θ_2 and ϕ_2 are the polar angle and azimuthal angle of the K meson in the $K\pi$ center of mass system.

where, the first error is statistical, the second error is systematic, the factor $\frac{1}{2}$ is because events are counted twice, $\frac{1}{9}$ is the isospin factor, and 2 is because the data comes from two decay channels: $J/\psi \rightarrow K^*(892)^+ K^*(892)^- \rightarrow (K^+\pi^0)(K_S\pi^-)$ and $J/\psi \rightarrow K^*(892)^- K^*(892)^+ \rightarrow (K^-\pi^0)(K_S\pi^+)$. The systematic error includes uncertainties from multi-solutions, from different background fit methods, and from removing some components from fit($K_0^*(1430)$, IPS, and $b_1(1235)$).

6 Summary

In conclusion, the charged κ is observed and studied in the decay $J/\psi \rightarrow K^*(892)^\pm \kappa^\mp \rightarrow K^\pm K_S \pi^\mp \pi^0$. The low mass enhancement in the $K\pi$ spectrum cannot be fit well unless a charged κ is added into the solution. If we use a Breit-Wigner function of constant width to parameterize the κ , its pole locates at $(849 \pm 77_{-14}^{+18}) - i(256 \pm 40_{-22}^{+46}) \text{ MeV}/c^2$. In our analysis, three different κ parameterizations are tried in the fit, and final results are shown in Table 3 and are consistent with those of the neutral κ and are also in good agreement with those obtained in the analysis of $K\pi$ scattering phase shifts. Also, the decay $J/\psi \rightarrow K^*(892)^\pm K^*(892)^\mp$ is observed for the first time with the branching ratio $(1.00 \pm 0.19_{-0.32}^{+0.11}) \times 10^{-3}$. The corresponding decay mode is not observed in $J/\psi \rightarrow \bar{K}^*(892)^0 K^+ \pi^-$. The decays $J/\psi \rightarrow K^*(892)^\pm K^*(892)^\mp$ can be produced through J/ψ electromagnetic decays, while $J/\psi \rightarrow K^*(892)^0 \bar{K}^*(892)^0$ can only be produced through J/ψ hadronic decays, which would be $SU(3)$ symmetry breaking decays and are suppressed.

Acknowledgments The BES Collaboration thanks the staff of BEPC and computing center for their hard efforts. This work is supported in part by the National Natural Science Foundation of China under contract Nos. 10491300, 10225524, 10225525, 10425523, 10625524, 10521003, 10821063, 10825524, the Chinese Academy of Sciences under contract No. KJ 95T-03, the 100 Talents Program of CAS under Contract Nos. U-11, U-24, U-25, and the Knowledge Innovation Project of CAS under contract Nos. U-602, U-34 (IHEP), the National Natural Science Foundation of China under contract Nos. 10775077, 10225522 (Tsinghua University), and the Department of Energy under Contract No. DE-FG02-04ER41291 (U. Hawaii).

References

- [1] Ning Wu (BES collaboration), "BES R measurements and J/ψ Decays", Proceedings of the XXXVIth Rencontres de Moriond, Les Arcs, France, March 17 – 24, 2001, Ed. J. Tran Thanh Van. 2001 QCD and High Energy Hadronic Interactions, p.3-6.
- [2] J.Z.Bai, BES Collaboration, hep-ex/0304001.
- [3] J.Z.Bai, et al., BES collaboration, High Energy Phys. Nucl. Phys. 28 (2004) 215.
- [4] M. Ablikim, et al., BES collaboration, Phys. Lett. **B 598** (2004) 149.
- [5] M. Ablikim, et al., BES collaboration, Phys. Lett. **B 645** (2007) 19.

- [6] M. Ablikim, et al., BES collaboration, Phys. Lett. **B 633** (2006) 681.
- [7] E.M. Aitala, et al., Fermilab E791 Collaboration, Phys. Rev. Lett. **86** (2001)770.
- [8] E.M. Aitala, et al., Fermilab E791 Collaboration, Phys. Rev. Lett. **89** (2002)121801.
- [9] D. Alde, et al., Phys. Lett **B 397** (1997) 350.
- [10] T. Ishida, et al., in: Proceedings of International Conference Hadron'95, World Scientific, Manchester, UK, 1995.
- [11] V.E. Markushin, M.P. Locher, Frascati Phys. ser. **15** (1999) 229.
- [12] Z.Xiao, H.Q.zheng, Nucl. Phys. **A 695** (2001) 273.
- [13] J.M. Link, et al., FNAL FOCUS Collaboration, Phys. Lett. **B535** (2002)430.
- [14] C. Cawfield, et al., CLEO Collaboration, Phys. Rev. **D 74** (2006) 031108R.
- [15] M.R. Shepherd, et al., CLEO Collaboration, Phys. Rev. **D 74** (2006) 052001.
- [16] D. Epifanov, et al., BELLE Collaboration, Phys. Lett. **B 654** (2007) 65.
- [17] S. Anderson, et al., Phys. Rev. **D 63** (2001)09001.
- [18] B. Aubert, et al., BABAR Collaboration, Phys. Rev. **D 76** (2007) 011102R.
- [19] E. van Beveren, et al., Z. Phys. **C 30** (1986)651.
- [20] D. Aston, et al., Nucl. Phys. **B 296** (1988)253.
- [21] S. Ishida, et al., Prog. Theor. Phys. **98** (1997)621.
- [22] D.Black, et al., Phys. Rev. **D58** (1998)054012
- [23] J.A. Oller, E. Oset, Phys. Rev. **D 60** (1999)074023.
- [24] M.J. Jamin, et al., Nucl. Phys. **B 587** (2000)331.
- [25] D. Bugg, Phys. Lett. **B 572** (2003)1.
- [26] H.Q.Zheng, et al., Nucl. Phys. **A 733** (2004) 235.
- [27] D. Lohs, Phys. Lett. **B 234** (1990)235.
- [28] N.A. Tornqvist, Z. Phys. **C 68** (1995) 467.
- [29] A.V. Anisovich, A.V. Sarantsev, Phys. Lett. **B 413** (1997) 137.
- [30] S.N. Cherry, M.R. Pennington, Nucl. Phys. **A 688** (2001) 823.
- [31] Particle Data Group, Phys. Lett. **B 667** (2008) 1.
- [32] J.Z. Bai, et al., BES Collaboration, Nucl. Instrum. Methods, **A 344** (1994)319;
J.Z. Bai, et al., BES Collaboration, Nucl. Instrum. Methods, **A 458** (2001)627.
- [33] M. Jacob, G.C. Wick, Ann.Phys. (NY) **7** 404 (1959).

- [34] S.U.Chung, Phys. Rev. D57, 1998:431-442.
- [35] Ning Wu and Tu-Nan Ruan, Commun. Theor. Phys. (Beijing, China) **35** (2001) 547.
- [36] Ning Wu and Tu-Nan Ruan, Commun. Theor. Phys. (Beijing, China) **35** (2001) 693.
- [37] Ning Wu and Tu-Nan Ruan, Commun. Theor. Phys. (Beijing, China) **37** (2002) 309.
- [38] H.Q. Zheng, *How to parameterize a resonance with finite width* , Talk given at International Symposium on Hadron Spectroscopy, Chiral Symmetry and Relativistic Description of Bound Systems, Tokyo, Japan, 24-26 Feb 2003; hep-ph/0304173.

